



Universidad Autónoma
de Madrid

Biblos-e Archivo
Repositorio Institucional UAM

Repositorio Institucional de la Universidad Autónoma de Madrid

<https://repositorio.uam.es>

Esta es la **versión de autor** del artículo publicado en:
This is an **author produced version** of a paper published in:

Angewandte Chemie International Edition 59 (2020): 9041–9046

DOI: <https://doi.org/10.1002/anie.201916261>

Copyright: © 2020 Wiley-VCH Verlag GmbH & Co. KGaA, Weinheim

El acceso a la versión del editor puede requerir la suscripción del recurso
Access to the published version may require subscription

Elucidating Noncovalent Reaction Mechanisms: Identification of the G-Quartet as an Intermediate in G-Quadruplex Assembly

Miguel Martín-Arroyo,^[a] Anselmo del Prado,^[a] Raquel Chamorro,^[a] Nerea Bilbao,^[a] and David González-Rodríguez^{[a,b]*}

[a] Dr. M. Martín-Arroyo, Dr. A. del Prado, Dr. R. Chamorro, Dr. N. Bilbao, Dr. D. González-Rodríguez
Nanostructured Molecular Systems and Materials (MSMn) Group, Departamento de Química Orgánica, Facultad de Ciencias
Institution
Universidad Autónoma de Madrid, 28049 Madrid, Spain
E-mail: david.gonzalez.rodriguez@uam.es

[b] Institute for Advanced Research in Chemical Sciences (IAdChem)
Universidad Autónoma de Madrid, 28049 Madrid, Spain

Supporting information for this article is given via a link at the end of the document.

Abstract: In analogy to covalent reactions, the understanding of noncovalent association pathways is fundamental to influence and control any supramolecular process. Following an approach that is reminiscent of covalent methodologies, we study here, for the first time, the mechanism of G-quadruplex formation in organic solvents. Our results support a reaction pathway in which the cation shifts first the equilibrium towards a G-quartet transient intermediate, which then acts as a template in the formation of the G-quadruplex product.

Introduction

In analogy to covalent reactions,^[1] supramolecular association processes can follow distinct mechanisms that involve transient intermediates, well-defined transition states and thermodynamic and kinetic products. The study and comprehension of such transformation pathways is fundamental to rationally influence a supramolecular process in terms of product yields, molecularity, selectivities and kinetic rates. A crucial limitation and difference with respect to kinetically controlled reactions is that noncovalent products are normally obtained under equilibrium control and exhibit short lifetimes when removed from these conditions.

Supramolecular reaction mechanisms have been classically studied for host-guest systems.^[2] Here, experimental analysis is simplified because of the presence of (at least) two species and the possibility of studying exchange processes between different guests and/or hosts, which afford valuable structure-kinetic relationships to verify a mechanistic proposal.^[3] More recently, attention has been focused on establishing and controlling reaction pathways in noncovalent polymerizations,^[4] which can rule helical chirality, the degree of polymerization, and the nature and morphology of the final nanomaterial.^[5] An increasing number of small molecules are found to assemble through concurrently competing kinetically and thermodynamically controlled processes,^[5] which in some instances resemble and help to understand complex protein aggregation mechanisms.^[6]

Independently of its covalent or noncovalent nature, one of the keys in determining a reaction mechanism is the identification of self-assembled *intermediates*, which may be detected by careful modification of the experimental conditions (temperature, concentration, solvent, stoichiometric ratios). Such species constitute local minima along the reaction pathway that in most

cases are too ephemeral to be sensed because they transform rapidly and/or their concentration is too small.^[7] In other instances, the structure of these intermediates can be deduced from kinetic products^[8] that are trapped operating under out-of-equilibrium conditions,^[3b,9] and that then evolve to the thermodynamic product under equilibrium control. Still, the identification of self-assembled intermediates is very rare and, in analogy again to covalent processes, these intermediates must be distinguished from *by-products*, which are thermodynamically stabilized secondary species that do not necessarily participate in the reaction itinerary leading to the target assembly.

In this work, we focus on the determination of self-assembly mechanisms following a protocol that is reminiscent of covalent methodologies: 1) consideration of a mechanistic proposal that is questioned to include a potential intermediate; 2) intermediate isolation and characterization under specific conditions; 3) identification of such species along product formation; 4) confirmation of its intermediate nature and hence of the reaction pathway proposed. For that goal, we selected guanine (G) self-assembly in organic solvents as a model supramolecular reaction to study, for the first time, the mechanism of G-quadruplex formation (Figure 1a).

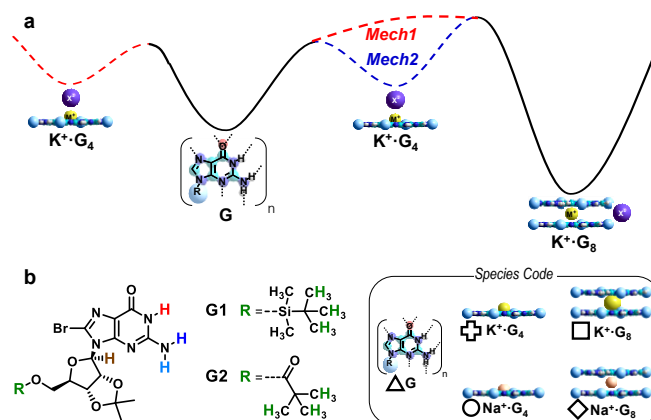


Figure 1. (a) Proposed supramolecular reaction pathway leading to a K^+ -G₈ octamer, without (*Mech1*) or with (*Mech2*) a G₄ quartet as an intermediate (b) Chemical structure of **G1** and **G2**. Proton and species codes used herein for ¹H NMR labelling are indicated with colours and geometric shapes, respectively.

Results and Discussion

G self-assembly constitutes an outstanding example of a supramolecular transformation.^[10] In organic solvents, G derivatives typically associate into loosely bound, rapidly exchanging hydrogen (H)-bonded oligomeric species (G_n ; Figure 1a). Now, in the presence of a size-matching cation (commonly Na^+ or K^+), multiple noncovalent forces work in concert to afford well-defined G-quadruplexes,^[11] the G-octamer (G_8 ; Figure 1a) being the most simple prototypical version. These assemblies are constituted by stacked H-bonded cyclic tetramers (G-quartets or G_4 ; Figure 1a) and display remarkable cooperativity and kinetic stability.^[11h] Besides its relevant natural role in telomere formation, G-quadruplex self-assembly is nowadays the basis of manifold applications in biological and materials sciences.^[12]

However, although the interconversion between different G-quadruplexes in equilibrium, namely G_8 , G_{12} and G_{16} , as a function of molecular structure and experimental conditions has been studied by several authors,^[11c-g,13] nothing is known about the early-stage pathway followed by G molecules along their noncovalent assembly in G-quadruplexes. How does the cation template the formation of a G-quadruplex? As a starting point, we propose two main supramolecular pathways that could be potentially involved in the formation of a G_8 quadruplex (Figure 1a). In the first one (*Mech1*, in red), the cation directly templates G_8 formation by octahedral coordination to G monomers or H-bonded oligomers in a concerted manner, without the participation of any particularly stabilized intermediate. In the second path (*Mech2*; in blue), the cation shifts the equilibrium between G-oligomers towards the cyclic G_4 complex, which becomes a stabilized intermediate species in the overall self-assembly landscape. Then, the metal-bound G-quartets may act as a template platform to yield G_8 . Here, we provide experimental evidence that strongly supports this second mechanistic postulate.

Compounds **G1**^[11e] and **G2**^[11h] (Figure 1b) self-assemble in the presence of K^+ salts, such as KPF_6 , KI, $KBPh_4$ or $KMeDNP$ ($MeDNP$ = 4-methyl-2,6-dinitrophenolate), into D_4 -symmetric octamers ($K^+ \cdot G_8$) in TCE- D_2 or THF- D_8 . We chose to work with 8-bromoguanosines due to our experience with this kind of derivatives and because they usually show higher solubility and provide sharper NMR signals than their unsubstituted analogues. In comparison to uncomplexed G (Figure 2a), in which, according to NMR data, a fast-exchanging equilibrium between small H-bonded oligomers is established, such K^+ complexes are characterized in 1H NMR by a sharp NH amide proton signal at 12.0 ppm in both solvents (Figure 2b). In addition, the NH_2 protons split into two new signals as the structure is stabilized and the C-N bond spinning freezes in the NMR timescale: the H-bonded proton in the quartet ($NH_2(b)$) at ca. 8–9 ppm and the solvent-exposed proton ($NH_2(f)$) at lower chemical shifts. This splitting is observed at 298 K in TCE- D_2 and below 283 K in the more polar THF- D_8 solvent (see Figure S1A). Moreover, while the $K^+ \cdot G_8$ complex displayed a remarkable stability to concentration changes in TCE, dilution of the THF samples results in quadruplex dissociation (Figure S1B–C) and a slow $K^+ \cdot G_8 - G$ equilibrium is established in 1H NMR, demonstrating the strong *all-or-none* cooperativity of this system. The formation of these charged complexes can also be characterized by ESI Q-TOF MS, in which, in contrast to the ill-defined, low intensity signals of uncomplexed G (Figure 2d), a high intensity $[G_8+K]^+$ peak (Figure 2e) is detected. On the other hand, DOSY NMR measurements

(Figures S1C–D) afforded a hydrodynamic radius of $R = 18.7$ Å, which matches the one obtained from computational models. Finally, the CD spectra of the $G_8 \cdot KBPh_4$ complex showed a negative Cotton effect (Figure 2h), in agreement with data reported for related G assemblies.^[14]

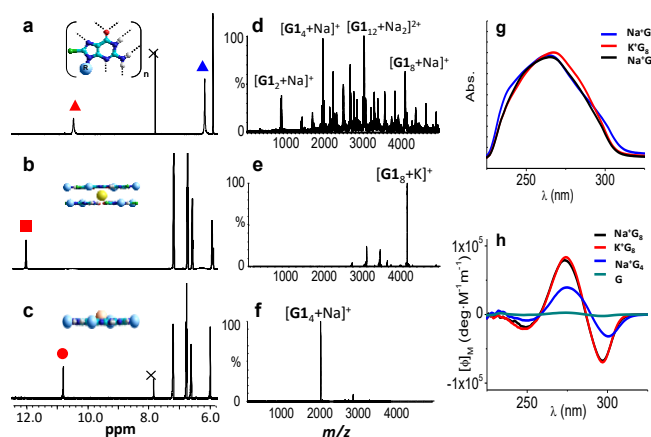


Figure 2. (a–c) Downfield region of the 1H NMR spectra in THF- D_8 at 298 K and (d–e) ESI Q-TOF MS spectra of **G1** in (a,d) the absence of cation, (b,e) the presence of $KBPh_4$ or (c,f) $NaBPh_4$. For proton and species codes, see Figure 1. (g) Absorption and (h) CD spectra of **G2** (G) and the 3 **G2** complexes in TCE.

Next, we made a screening of different conditions, including cation, anion, solvent and concentration, with the aim of obtaining our hypothetical intermediate in solution: a complexed G-quartet. However, due to the strong preference for sandwiched complexes with octahedral coordination to the carbonyl groups, particularly in the case of the larger K^+ cation (1.38 Å), the unambiguous detection of the G-quartet, in equilibrium in solution with other G-quadruplexes, has never been achieved. For the same reason, the stabilization of isolated G-quartets has been rarely observed.^[15] Cation-free or Na^+ -bound quartets have only been characterized in the crystal^[15a,b] or gas phases,^[15c] or using covalent^[15d–h] and noncovalent^[15i] templates.

On the basis of our experience and literature data, we reasoned that the smaller size of the Na^+ cation (1.02 Å) and the use of a large counteranion, such as BPh_4^- , are more suited to produce non-stacked G_4 species. In fact, the complexation of **G1/G2** in the presence of a small excess of $NaBPh_4$ salts led to a single species that displayed a sharp NH proton signal at 10.8 (THF- D_8 ; Figure 2c) or 11.4 ppm (TCE- D_2 , see below). Upon dilution of the THF samples (Figure S2A), a new broad NH signal, characteristic of free G, grows at the expense of the original sharp signal, which confirms the supramolecular nature of this new $Na^+ \cdot G_4$ species. The $Na^+ \cdot G_4 - G$ equilibrium was found to be slow in the NMR timescale at 298 K in TCE- D_2 , but only at temperatures below 278 K in THF- D_8 , which underlines the lower kinetic stability of this complex when compared to the $K^+ \cdot G_8$ quadruplex. Moreover, ESI Q-TOF MS (Figure 2f) revealed a prominent peak corresponding to the $[G_4+Na]^+$ ion, whereas DOSY NMR showed a single diffusing species with a hydrodynamic radius of 17.3 Å (Figure S2B), slightly lower than that determined for $K^+ \cdot G_8$. The absorption and CD signatures (Figures 2g–h) of $Na^+ \cdot G_4$ are similar, but less intense and slightly red-shifted with respect to $K^+ \cdot G_8$, which is attributed to its non-stacked nature.^[16] Although further experiments, in combination with theoretical calculations, would be required to understand the origin of the CD signal in this non-stacked species, other G-

RESEARCH ARTICLE

quartets formed by the use of covalent templates^[15f,g,17a] and other non-stacked cyclic nucleoside structures^[17b-f] have also show relatively intense CD activity.

It is interesting to remark that the formation of the **G1/G2** quartet was only observed in these conditions in the presence of NaBPh₄ or, less reliably, NaMeDNP. Any K⁺ salt or the use of other counteranions, like NaPF₆ or NaI, resulted in the formation of octameric complexes, most commonly characterized by sharp amide signals around 12.0. In line with our previous work,^{11e,12a} we believe that the size of the anion plays an important role in preventing the formation of stacked quadruplexes. On the other hand, complexation with NaBPh₄ in CDCl₃ led again to octameric species whereas the use of more polar solvents, like acetone or acetonitrile, produced mixtures of dodecamer and hexadecamer quadruplexes (see also ref. 11e). This suggests that the THF and TCE solvents play also a crucial role in stabilizing the G-quartet.

Once the experimental conditions for the characterization of the postulated G₄ intermediate were identified, at least as a Na⁺ complex, we studied the progressive transformations between G assemblies in equilibrium as a function of the amount and nature of cation added. We specifically monitored the changes observed in 4 regions of the ¹H NMR spectra of **G2** as increasing amounts of KBPh₄/NaBPh₄ salt were added (Figures 3 and S3). Due to the slow exchange observed in the NMR timescale in TCE-D₂, the formation of each complex can be quantified along these titrations. Figure 3a shows the gradual formation of K⁺·G₈, evidenced in the characteristic sharp NH proton at 12.0 ppm, the (NH₂(b)) proton signal at 8.3 ppm, and also in a shift of the *t*-Bu proton signals from 1.19 to 1.26 ppm. No other species (for instance, the sought K⁺·G₄ complex) were detected along this experiment. Now, when the same titrations are performed with NaBPh₄, a different outcome was found (Figure 3c). At low salt equivalents, a new species evolves that exhibits a broad NH signal at 12.3 ppm (that sharpens at higher temperatures; see Figure S4C) and NH₂(b) and *t*-Bu proton signals at 8.1 and 1.24 ppm. We assign these new features to the NaBPh₄·G₈ complex due to the fact that it is formed close to quantitatively at exactly an 8:1 **G2**:Na⁺ ratio. Besides, DOSY analysis afforded a larger hydrodynamic radius (*R* = 18.2 Å; Figure S2C) than G₄, comparable to the one found for G₈, while the CD spectra was virtually superimposable to that of K⁺·G₈ (Figure 2h). Interestingly, when higher amounts of Na⁺ salt are added, these features now evolve to a sharp NH signal at 11.4 ppm, and NH₂(b) and *t*-Bu proton signals at 8.8 and 1.27 ppm, which are attributed to the Na⁺·G₄ quartet, as described above.

It is interesting to note that this Na⁺·G₄ species can be then transformed to K⁺·G₈ by gradual addition of KBPh₄ (Figure 3b). After adding a small excess of this salt, the broad ¹H NMR features previously assigned to Na⁺·G₈ were again observed, an experimental finding for which we don't have a clear explanation, although they readily disappear at the expense of the K⁺·G₈ signals above 1/16 KBPh₄ equivalents. These results evidence the strong preference of G for complexing K⁺ over Na⁺ salts.

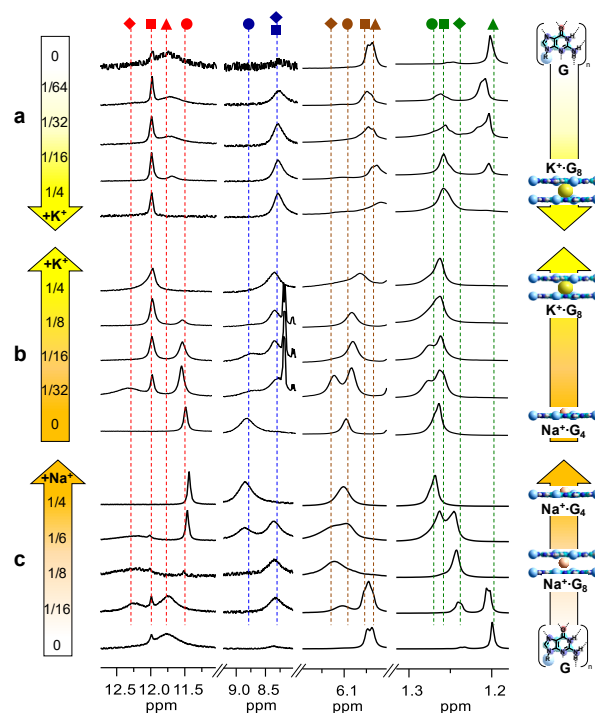


Figure 3. Evolution of 4 distinct ¹H NMR regions (from left to right: NH, NH₂(b), C1'-H, and *t*-Bu proton regions) of **G2** in TCE-D₂ (298 K; 10⁻¹ M) as increasing equivalents of (a,b) KBPh₄ or (c) NaBPh₄ are added over (a,c) uncomplexed **G2** or (b) **G2** + 1/4 eqs. of NaBPh₄. For proton and species codes see Figure 1.

Once the characteristic NMR features of the G₈ and G₄ complexes, as well as their relationships at different G:salt ratios were established, we designed a series of experiments that could demonstrate or discard the eventual participation of the G-quartet in G-quadruplex formation. In contrast to kinetically controlled reactions, supramolecular systems present the characteristic that, even if the reaction is finished and the equilibrium established, reactants and products are constantly under dynamic exchange, so association and dissociation pathways can still be investigated.

A first key experiment consisted in trying to detect the K⁺·G₄ quartet (which has been so far not characterized, but we assume it should have similar features to Na⁺·G₄) in equilibrium with the K⁺·G₈ octamer. To this end, we carried out variable temperature experiments in conditions where K⁺-complexed and uncomplexed G species are present in slow equilibrium (10⁻² M in THF-D₈; see Figure S1B). Upon cooling (Figure 4a), the K⁺·G₈ proton signals undergo the same trends seen at higher concentrations (Figure S1A): the splitting of the NH₂ signals was observed below 283 K while its concentration increases, as evidenced for instance in the relative ratio of the ribose proton signals. On the other hand, the broader NH signal of free G experiences an upfield shift as the temperature is decreased, which is indicative of a higher involvement in H-bonding. However, just below 278 K, this species originates a sharp new signal close to 11.0 ppm, that also grows at the expense of free G at lower temperatures. We attribute this signal to the K⁺·G₄ quartet, which at high temperatures is in fast equilibrium with uncomplexed G, and at low temperatures becomes kinetically stabilized, as previously observed for Na⁺·G₄ in THF-D₈. These two species are, at the same time, in slow exchange with the K⁺·G₈ octamer, independently on concentration or temperature. It is important to note that the K⁺·G₄ NH₂ signals experience the same kind of

RESEARCH ARTICLE

splitting than those of $\text{K}^+\cdot\text{G}_8$, but at much lower temperatures (*i.e.* below 223 K), reflecting the lower stability of this complex. Finally, in order to compare the relative size of this two K^+ complexes in slow exchange, DOSY experiments were performed at 233 K (Figure 4b), which revealed that the $\text{K}^+\cdot\text{G}_8$ proton signals appear at lower diffusion coefficients than the $\text{K}^+\cdot\text{G}_4$ signals.

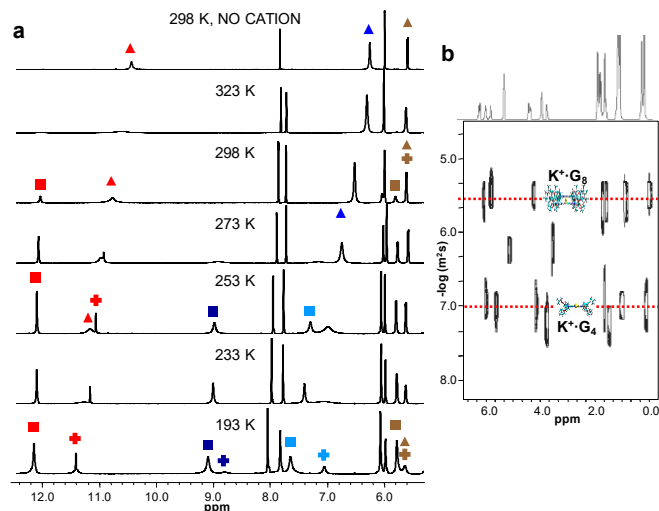


Figure 4. (a) ^1H NMR spectra of **G1** in $\text{THF-}D_8$ ($[\text{G1}] = 10^{-2}$ M; +1/4 KMeDNP) as a function of the temperature. (b) Aliphatic region of the DOSY NMR spectra of **G1** ($[\text{G1}] = 10^{-2}$ M; $T = 233$ K) in the presence of KMeDNP and calculated radii. For proton and species codes, see Figure 1.

These experiments demonstrate that the (previously undetected) $\text{K}^+\cdot\text{G}_4$ quartet is indeed participating in the equilibrium between $\text{K}^+\cdot\text{G}_8$ and free **G**, but do not unambiguously reveal if this weaker complex is a side by-product (*Mech1*) or an actual intermediate in the association pathway (*Mech2*). In order to discern between these two situations, kinetic experiments in which $\text{K}^+\cdot\text{G}_8$ formation is monitored with time were next performed (Figure 5). A number of experimental conditions, including solvent, salt equivalents, and temperature were tested to optimize this challenging experiment. Unfortunately, the transformation of **G** into $\text{K}^+\cdot\text{G}_8$ was too fast for ^1H NMR acquisition in $\text{THF-}D_8$, but could be controlled and monitored in the relevant NH, $\text{NH}_2(\text{b})$ and *t*-Bu regions, at the expense of signal broadening, along the course of several minutes at low temperatures in $\text{TCE-}D_2$.

As shown in Figure 5a, just after mixing a 10^{-2} M solution of **G2** and 1/4 eqs. of KBPh_4 at 253 K, two new set of signals are detected. The first one, showing respectively NH, $\text{NH}_2(\text{b})$ and *t*-Bu proton signals at 12.0, 8.2 and 1.22 was attributed to $\text{K}^+\cdot\text{G}_8$ according to the previous results (Figure 3). The second one, displaying $\text{NH}_2(\text{b})$ and *t*-Bu proton signals at 8.8 and 1.27 ppm was ascribed to the $\text{K}^+\cdot\text{G}_4$ tetramer, due to the almost perfect match with the $\text{Na}^+\cdot\text{G}_4$ complex (shown on top in Figure 5a). The amide NH proton of $\text{K}^+\cdot\text{G}_4$, however, was not clearly detected, certainly not at the same chemical shift as in $\text{Na}^+\cdot\text{G}_4$. In view of all experiments performed (see also Figure S5), we believe it overlaps the $\text{K}^+\cdot\text{G}_8$ NH proton. The stronger differences in chemical shift between $\text{Na}^+\cdot\text{G}_4$ and $\text{K}^+\cdot\text{G}_4$ NH protons might be due its proximity to the Na^+ or K^+ -coordinated carbonyl group.

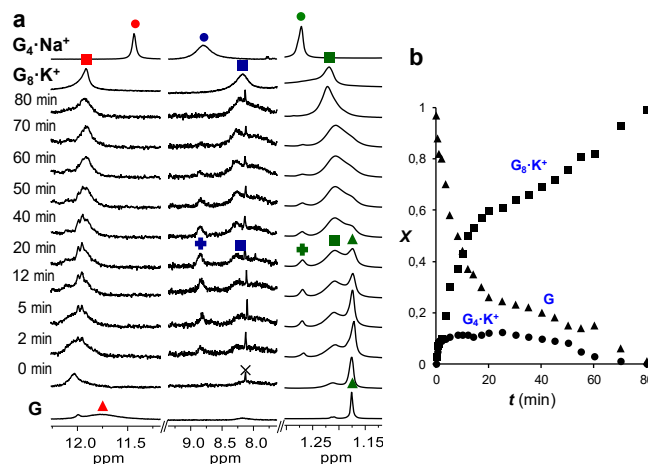


Figure 5. (a) Evolution of the NH, $\text{NH}_2(\text{b})$, and *t*-butyl ^1H NMR regions as a function of time after mixing $\text{TCE-}D_2$ solutions of **G2** and KBPh_4 (1/4 eqs) at 253 K. The spectra of free **G**, $\text{G}_4\cdot\text{Na}^+$ and $\text{G}_8\cdot\text{K}^+$ is shown for comparison. For proton and species codes, see Figure 1. (b) Changes in the molar fraction (χ) of free **G**, $\text{G}_4\cdot\text{K}^+$ and $\text{G}_8\cdot\text{K}^+$ with time.

The relative population of these three species was calculated by integration and displayed in Figure 5b as a function of time. Complex $\text{K}^+\cdot\text{G}_8$ begins to form gradually at the expense of free **G**, until the equilibrium is reached after ca. 120 minutes and $\text{K}^+\cdot\text{G}_8$ is formed quantitatively. The $\text{K}^+\cdot\text{G}_4$ complex, however, begins to form just upon mixing, then reaches a maximum abundance, not higher than 10%, and then its concentration decreases together with free **G** until it is no longer detected by ^1H NMR after about 60 mins. It is important to remark that both $\text{NH}_2(\text{b})$ and *t*-Bu proton probes show the same time evolution, and that the disappearance of the transient $\text{K}^+\cdot\text{G}_4$ complex is coupled to that of free **G**, to form the thermodynamically stabilized $\text{K}^+\cdot\text{G}_8$ species. Moreover, experiments performed at different salt ratios at 298 K showed qualitatively the same results, although kinetics are considerably faster and the $\text{K}^+\cdot\text{G}_4$ complex is no longer detected after 8 minutes, with a maximum relative abundance of ca. 1% (see Figure S5).

Conclusion

In conclusion, in this work we confronted the study of the mechanism of a key self-assembly process that differs from the classical supramolecular polymerization and host-guest systems: G-quadruplex association in organic solvents. We particularly focused on detecting the $\text{K}^+\cdot\text{G}_4$ quartet as an intermediate along $\text{K}^+\cdot\text{G}_8$ octamer formation following a protocol that resembles the study of covalent reaction mechanisms. We first reached experimental conditions in which the proposed G_4 intermediate is formed, although in its Na^+ -bound form, and studied the equilibrium relationships with G_8 complexes and uncomplexed **G**, which afforded the unambiguous characterization of the $\text{Na}^+\cdot\text{G}_4$ and $\text{Na}^+\cdot\text{G}_8$ species. We then designed several experiments in which the unprecedented $\text{K}^+\cdot\text{G}_4$ quartet could be detected in equilibrium and as a transient species along G-quadruplex formation. Our results support a mechanism in which the K^+ cation shifts the equilibrium between H-bonded G-oligomers towards a $\text{K}^+\cdot\text{G}_4$ cyclic complex, an intermediate that may then act as a template platform for further incorporation of **G** monomers or directly stack to yield the $\text{K}^+\cdot\text{G}_8$ thermodynamic product.

Acknowledgements

Funding from the European Research Council (ERC-Starting Grant 279548 PROGRAM-NANO) and MINECO (CTQ2014-57729-P and CTQ2017-84727-P) is gratefully acknowledged. M.M.-A. is grateful to MINECO for an FPI Grant (BES-2015-071795). A.dP. acknowledges a Marie Skłodowska-Curie Grant (843090).

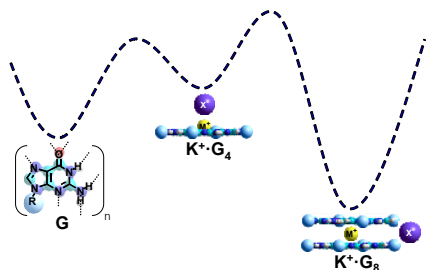
Keywords: Supramolecular Chemistry • Noncovalent Synthesis • G-quadruplex • Guanine Self-assembly • G-quartets

- [1] R. Bruckner, *Advanced Organic Chemistry: Reaction Mechanisms*, Elsevier, **2001**.
- [2] M. D. Pluth, K. N. Raymond, *Chem. Soc. Rev.* **2007**, *36*, 161-171.
- [3] a) C. Marquez, W. M. Nau, *Angew. Chem. Int. Ed.* **2001**, *40*, 3155-3160; *Angew. Chem.* **2001**, *113*, 3248-3254. b) J. C. Chapin, M. Kvasnica, B. W. Purse, *J. Am. Chem. Soc.* **2012**, *134*, 15000-15009; c) C. M. Hong, D. M. Kaphan, R. G. Bergman, K. N. Raymond, F. D. Toste, *J. Am. Chem. Soc.* **2017**, *139*, 8013-8021.
- [4] a) T. Aida, E. Meijer, S. I. Stupp, *Science* **2012**, *335*, 813-817; b) D. van der Zwaag, T. F. de Greef, E. Meijer, *Angew. Chem. Int. Ed.* **2015**, *54*, 8334-8336; *Angew. Chem.* **2015**, *127*, 8452-8454; c) C. Kulkarni, E. Meijer, A. R. Palmans, *Acc. Chem. Res.* **2017**, *50*, 1928-1936; d) A. Sorrenti, J. Leira-Iglesias, A. J. Markvoort, T. F. de Greef, T. M. Hermans, *Chem. Soc. Rev.* **2017**, *46*, 5476-5490; e) R. Otter, P. Besenius, *Org. Biomol. Chem.* **2019**, *17*, 6719-6734; f) J. Matern, Y. Dorca, L. Sánchez, G. Fernandez, *Angew. Chem. Int. Ed.* **2019**, *58*, 2-13; *Angew. Chem.* **2019**, *131*, 2-14.
- [5] a) P. A. Korevaar, C. J. Newcomb, E. Meijer, S. I. Stupp, *J. Am. Chem. Soc.* **2014**, *136*, 8540-8543; b) A. Aliprandi, M. Mauro, L. De Cola, *Nat. Chem.* **2016**, *8*, 10-15; c) T. Fukui, S. Kawai, S. Fujinuma, Y. Matsushita, T. Yasuda, T. Sakurai, S. Seki, M. Takeuchi, K. Sugiyasu, *Nat. Chem.* **2017**, *9*, 493-499; d) K. Cai, J. Xie, D. Zhang, W. Shi, Q. Yan, D. Zhao, *J. Am. Chem. Soc.* **2018**, *140*, 5764-5773; e) M. Wehner, M. I. S. Röhr, M. Bühler, V. Stepanenko, W. Wagner, F. Würthner, *J. Am. Chem. Soc.* **2019**, *141*, 6092-6107; f) L. Herkert, J. Droste, K. K. Kartha, P. A. Korevaar, T. F. de Greef, M. R. Hansen, G. Fernandez, *Angew. Chem. Int. Ed.* **2019**, *58*, 11344-11349; *Angew. Chem.* **2019**, *131*, 11466-11471.
- [6] a) J. Zhai, T.-H. Lee, D. H. Small, M.-I. Aguilar, *Biochemistry* **2012**, *51*, 1070-1078; b) M. Medrano, M. A. Fuertes, A. Valbuena, P. J. Carrillo, A. Rodríguez-Huete, M. G. Mateu, *J. Am. Chem. Soc.* **2016**, *138*, 15385-15396; c) T. C. Michaels, L. X. Liu, S. Curk, P. G. Bolhuis, A. Šarić, T. P. Knowles, *Mol. Phys.* **2018**, *116*, 3055-3065.
- [7] a) J. Chen, S. Körner, S. L. Craig, D. M. Rudkevich, J. Rebek Jr, *Nature* **2002**, *415*, 385-386; b) A. V. Davis, K. N. Raymond, *J. Am. Chem. Soc.* **2005**, *127*, 7912-7919; c) W. Jiang, D. Ajami, J. Rebek Jr, *J. Am. Chem. Soc.* **2012**, *134*, 8070-8073; d) Y. Nito, H. Adachi, N. Toyoda, H. Takaya, K. Kobayashi, M. Yamanaka, *Chem. Asian J.* **2014**, *9*, 1076-1082; e) A. Baba, T. Kojima, S. Hiraoka, *J. Am. Chem. Soc.* **2015**, *137*, 7664-7667.
- [8] a) H. Cui, Z. Chen, S. Zhong, K. L. Wooley, D. J. Pochan, *Science* **2007**, *317*, 647-650; b) V. M. Cangelosi, T. G. Carter, L. N. Zakharov, D. W. Johnson, *Chem. Commun.* **2009**, 5606-5608; c) F. Aparicio, B. Nieto-Ortega, F. Nájera, F. J. Ramírez, J. T. López Navarrete, J. Casado, L. Sánchez, *Angew. Chem. Int. Ed.* **2014**, *53*, 1373-1377; *Angew. Chem.* **2014**, *126*, 1397-1401.
- [9] a) P. A. Korevaar, S. J. George, A. J. Markvoort, M. M. Smulders, P. A. Hilbers, A. P. Schenning, T. F. De Greef, E. Meijer, *Nature* **2012**, *481*, 492; b) O. Danylyuk, V. P. Fedin, V. Sashuk, *Chem. Commun.* **2013**, *49*, 1859-1861; c) S. Saha, J. Bachl, T. Kundu, D. D. Díaz, R. Banerjee, *Chem. Commun.* **2014**, *50*, 7032-7035; d) Y. Guo, Y. Liu, Y. Gong, W. Xiong, C. Zhang, J. Zhao, Y. Che, *Chem. Eur. J.* **2019**, *25*, 7463-7468.
- [10] a) J. T. Davis, *Angew. Chem. Int. Ed.* **2004**, *43*, 668-698; *Angew. Chem. Int. Ed.* **2004**, *116*, 684-716; b) J. T. Davis, G. P. Spada, *Chem. Soc. Rev.* **2007**, *36*, 296-313; c) L. Stefan, D. Monchaud, *Nat. Rev. Chem.* **2019**, *3*, 650-668.
- [11] a) X. Shi, K. M. Mullaugh, J. C. Fetting, Y. Jiang, S. A. Hofstadler, J. T. Davis, *J. Am. Chem. Soc.* **2003**, *125*, 10830-10841; b) L. Ma, M. Iezzi, M. S. Kaucher, Y.-F. Lam, J. T. Davis, *J. Am. Chem. Soc.* **2006**, *128*, 15269-15277; c) M. d. C. Rivera-Sánchez, I. Andújar-de-Santis, M. García-Arriaga, V. Gubala, G. Hobbey, J. M. Rivera, *J. Am. Chem. Soc.* **2009**, *131*, 10403-10405; d) J. E. Betancourt, M. Martín-Hidalgo, V. Gubala, J. M. Rivera, *J. Am. Chem. Soc.* **2009**, *131*, 3186-3188; e) D. González-Rodríguez, J. L. J. van Dongen, M. Lutz, A. L. Spek, A. P. H. J. Schenning, E. W. Meijer, *Nat. Chem.* **2009**, *1*, 151-155; f) M. Martín-Hidalgo, J. M. Rivera, *Chem. Commun.* **2011**, *47*, 12485-12487; g) K. B. Sutyak, P. Y. Zavalij, M. L. Robinson, J. T. Davis, *Chem. Commun.* **2016**, *52*, 11112-11115; h) E. Fadaei, M. Martín-Arroyo, M. Tafazzoli, D. González-Rodríguez, *Org. Lett.* **2017**, *19*, 460-463.
- [12] a) D. González-Rodríguez, P. G. A. Janssen, R. Martín-Rapún, I. D. Cat, S. D. Feyter, A. P. H. J. Schenning, E. W. Meijer, *J. Am. Chem. Soc.* **2010**, *132*, 4710-4719; b) Y.-L. Wu, K. E. Brown, D. M. Gardner, S. M. Dyar, M. R. Wasielewski, *J. Am. Chem. Soc.* **2015**, *137*, 3981-3990; c) M. García-Iglesias, T. Torres, D. González-Rodríguez, *Chem. Commun.* **2016**, *52*, 9446-9449; d) G. M. Peters, J. T. Davis, *Chem. Soc. Rev.* **2016**, *45*, 3188-3206; e) Y.-L. Wu, N. E. Horwitz, K.-S. Chen, D. A. Gomez-Gualdrón, N. S. Luu, L. Ma, T. C. Wang, M. C. Hersam, J. T. Hupp, O. K. Farha, R. Q. Snurr, M. R. Wasielewski, *Nat. Chem.* **2016**, *9*, 466-472; f) P. Pathak, W. Yao, K. D. Hook, R. Vik, F. R. Winnerdy, J. Q. Brown, B. C. Gibb, Z. F. Pursell, A. T. Phan, J. Jayawickramarajah, *J. Am. Chem. Soc.* **2019**, *141*, 12582-12591.
- [13] a) M. García-Arriaga, G. Hobbey, J. M. Rivera, *J. Org. Chem.* **2016**, *81*, 6026-6035; b) D. Silva-Brenes, L. Delgado, J. M. Rivera, *Org. Biomol. Chem.* **2017**, *15*, 782-786.
- [14] L. Meng, K. Liu, S. Mo, Y. Mao, T. Yi, *Org. Biomol. Chem.* **2013**, *11*, 1525-1532.
- [15] a) J. L. Sessler, M. Sathiosatham, K. Doerr, V. Lynch, K. A. Abboud, *Angew. Chem. Int. Ed.* **2000**, *39*, 1300-1303; *Angew. Chem.* **2000**, *112*, 1356-1359; b) Y. Inui, M. Shiro, S. Fukuzumi, T. Kojima, *Org. Biomol. Chem.* **2013**, *11*, 758-764; c) C. Fraschetti, M. Montagna, L. Guarcini, L. Guidoni, A. Filippi, *Chem. Commun.* **2014**, *50*, 14767-14770; d) F. W. Kotch, V. Sidorov, Y.-F. Lam, K. J. Kayser, H. Li, M. S. Kaucher, J. T. Davis, *J. Am. Chem. Soc.* **2003**, *125*, 15140-15150; e) M. Nikan, J. C. Sherman, *Angew. Chem. Int. Ed.* **2008**, *47*, 4900-4902; *Angew. Chem.* **2008**, *120*, 4978-4980; f) M. Nikan, J. C. Sherman, *J. Org. Chem.* **2009**, *74*, 5211-5218; g) G. A. L. Bare, B. Liu, J. C. Sherman, *J. Am. Chem. Soc.* **2013**, *135*, 11985-11989; h) A. Laguerre, L. Stefan, M. Larouy, D. Genest, J. Novotna, M. Pirrotta, D. Monchaud, *J. Am. Chem. Soc.* **2014**, *136*, 12406-12414; i) Y. Inui, S. Fukuzumi, T. Kojima, *Dalton T.* **2013**, *42*, 3779-3782.
- [16] A. Randazzo, G. P. Spada, M. W. da Silva, *Top. Curr. Chem.* **2013**, *330*, 67-86.
- [17] a) P. Murat, B. Gennaro, J. Garcia, N. Spinelli, P. Dumy, E. Defrancq, *Chem. Eur. J.* **2011**, *17*, 5791-5795; b) C. Montoro-García, J. Camacho-García, A. M. López - Pérez, N. Bilbao, S. Romero-Pérez, M. J. Mayoral, D. González - Rodríguez, *Angew. Chem. Int. Ed.* **2015**, *54*, 6780-6784; b) S. Romero-Pérez, J. Camacho-García, C. Montoro-García, A. M. López-Pérez, A. Sanz, J. C. Mayoral, D. González-Rodríguez, *Org. Lett.* **2015**, *17*, 2664-2667; c) C. Montoro-García, J. Camacho-García, A. M. López-Pérez, M. J. Mayoral, N. Bilbao, D. González-Rodríguez, *Angew. Chem. Int. Ed.* **2016**, *55*, 223-227; d) C. Montoro-García, M. J. Mayoral, R. Chamorro, D. González-Rodríguez, *Angew. Chem.* **2017**, *129*, 15855-15859; e) M. J. Mayoral, D. Serrano-Molina, J. Camacho-García, E. Magdalena-Estirado, M. Blanco-Lomas, E. Fadaei, D. González-Rodríguez, *Chem. Sci.* **2018**, *9*, 7809-7821.

Entry for the Table of Contents

Elucidating Noncovalent Reaction Mechanisms: Identification of the G-Quartet as an Intermediate in G-Quadruplex Assembly

Miguel Martín-Arroyo, Anselmo del Prado, Raquel Chamorro, Nerea Bilbao, David González-Rodríguez*



A transient K⁺ G-quartet has been detected as an intermediate along the course of G-quadruplex self-assembly following an approach that is reminiscent of classical covalent mechanistic studies.

Researcher Twitter usernames: @miguel_getafe, @PolyAnsel, @DGRIlab

Institute Twitter username: @UOrganicchem